Biochimica et Biophysica Acta 1837 (2014) 1781–1789

Contents lists available at ScienceDirect

Biochimica et Biophysica Acta

journal homepage: www.elsevier.com/locate/bbabio

Cytotoxicity of mitochondria-targeted resveratrol derivatives: Interactions with respiratory chain complexes and ATP synthase

Nicola Sassi [a,b], Andrea Mattarei [b,c], Michele Azzolini [a], Ildiko' Szabo' [d], Cristina Paradisi [c], Mario Zoratti [a,b], Lucia Biasutto [a,b,*]

[a] Department of Biomedical Sciences, Viale G. Colombo 3, 35121 Padova, Italy
[b] CNR Neuroscience Institute, Viale G. Colombo 3, 35121 Padova, Italy
[c] Department of Chemical Sciences, Via F. Marzolo 1, 35131 Padova, Italy
[d] Department of Biology, Viale G. Colombo 3, 35121 Padova, Italy

ARTICLE INFO

Article history:
Received 28 December 2013
Received in revised form 13 June 2014
Accepted 27 June 2014
Available online 2 July 2014

Keywords:
Resveratrol
Triphenylphosphonium
ROS
Mitochondria
Respiratory chain
ATP synthase

ABSTRACT

We recently reported that mitochondria-targeted derivatives of resveratrol are cytotoxic in vitro, selectively inducing mostly necrotic death of fast-growing and tumoral cells when supplied in the low μM range (N. Sassi et al., Curr. Pharm. Des. 2014). Cytotoxicity is due to H_2O_2 produced upon accumulation of the compounds into mitochondria. We investigate here the mechanisms underlying ROS generation and mitochondrial depolarization caused by these agents. We find that they interact with the respiratory chain, especially complexes I and III, causing superoxide production. "Capping" free hydroxyls with acetyl or methyl groups increases their effectiveness as respiratory chain inhibitors, promoters of ROS generation and cytotoxic agents. Exposure to the compounds also induces an increase in the occurrence of short transient [Ca^{2+}] "spikes" in the cells. This increase is unrelated to ROS production, and it is not the cause of cell death. These molecules furthermore inhibit the F_0F_1 ATPase. When added to oligomycin-treated cells, the acetylated/methylated ones cause a recovery of the cellular oxygen consumption rates depressed by oligomycin. Since a protonophoric futile cycle which might account for the uncoupling effect is impossible, we speculate that the compounds may cause the transformation of the ATP synthase and/or respiratory chain complex(es) into a conduit for uncoupled proton translocation. Only in the presence of excess oligomycin the most effective derivatives appear to induce the mitochondrial permeability transition (MPT) within the cells. This may be considered to provide circumstantial support for the idea that the ATP synthase is the molecular substrate for the MPT pore.

© 2014 Elsevier B.V. All rights reserved.

1. Introduction

Cancer cells have an altered redox homeostasis [1–5] and hyperpolarized mitochondria [6–9]. This latter characteristic is a consequence of the shift from mitochondrial respiration to aerobic glycolytic ATP synthesis (the so-called Warburg effect), which leads to reduced oxidative phosphorylation activity, less efficient dissipation of the mitochondrial electrochemical proton gradient, and thus to an increased transmembrane potential [6,8]. ROS-generating agents targeted to mitochondria thanks to conjugation with lipophilic cations (which accumulate in the mitochondrial matrix according to the Nerst's law) have thus been developed, and are emerging as a promising class of mitocans, i.e., anticancer agents acting on mitochondria and destabilizing them [10,11]. Mitochondrial hyperpolarization leads to preferential accumulation of the pro-oxidant agents in cancer cells. Furthermore, the additional oxidative stress they cause may push cancerous cells over the brink of death more easily than normal cells [2–5]. A recent paper has indeed shown that healthy primary B cells can be sensitized to certain pro-apoptotic drugs by induction of a mild mitochondrial oxidative stress with a mitochondriotropic quercetin derivative. Conversely, cancerous

Abbreviations: B-CLL, B-cell chronic lymphocytic leukemia; BSA, bovine serum albumin; BTPI, 4-triphenylphosphoniumbutyl; CoQ, coenzyme Q; CsA, cyclosporin A; DCPI, 2,6-dichlorophenolindophenol; $\Delta\psi_m$, mitochondrial membrane potential; DMEM, Dulbecco's Modified Eagle Medium; $\Delta\tilde{\mu}_H$, proton electrochemical gradient; ECAR, extracellular acidification rate; FACS, fluorescence-activated cell scanner; FBS, fetal bovine serum; FCCP, carbonyl cyanide p-trifluoromethoxy-phenylhydrazone; HBSS, Hank's Balanced Salt Solution; H_2DCF-DA, 2′,7′-dichlorodihydrofluorescein-diacetate; IMM, inner mitochondrial membrane; LDH, lactate dehydrogenase; MPT, mitochondrial permeability transition; OCR, oxygen consumption rate; OL, oligomycin; PEG-SOD, polyethyleneglycol-superoxide dismutase; PEG-CAT, polyethyleneglycol-catalase; PEP, phosphoenolpyruvate; PK, pyruvate kinase; R-4′BTPI, 4′-(4-triphenylphosphoniumbutyl) resveratrol iodide; R-3BTPI, 3-(4-triphenylphosphoniumbutyl) resveratrol iodide; RDA-4′BTPI, 3,5-diacetyl-4′-(4-triphenylphosphoniumbutyl) resveratrol iodide; RDA-3BTPI, 4′,5-diacetyl-3-(4-triphenylphosphoniumbutyl) resveratrol iodide; RDM-4′BTPI, 3,5-dimethyl-4′-(4-triphenylphosphoniumbutyl) resveratrol iodide; RDM-3BTPI, 4′,5-dimethyl-3-(4-triphenylphosphoniumbutyl) resveratrol iodide; RLM, rat liver mitochondria; ROI, regions of interest; ROS, reactive oxygen species; MTT, 3-(4,5-dimethylthiazol-2-yl)-2,5-diphenyltetrazolium bromide

* Corresponding author at: CNR Neuroscience Institute, Viale G. Colombo 3, 35121 Padova, Italy. Tel.: +39 049 8276483; fax: +39 049 8276040.
E-mail address: lucia.biasutto@cnr.it (L. Biasutto).

http://dx.doi.org/10.1016/j.bbabio.2014.06.010
0005-2728/© 2014 Elsevier B.V. All rights reserved.

B-CLL cells lose their peculiar sensitivity to the same drugs if treated with permeant ROS scavengers PEG-SOD and PEG-CAT [5].

We previously reported the synthesis and *in vitro* activity of a group of resveratrol derivatives targeted to mitochondria via a 4-triphenylphosphoniumbutyl (BTPI) group O-linked at either position -3 or -4′ [12,13]. These derivatives, in the low-μM range, induced necrotic cell death, selectively killing cancerous and fast-growing cells *in vitro* [13]. Resveratrol itself has previously been shown to be cytotoxic, but only at much higher doses (tens of μM) [14]. Mitochondrial targeting thus appears to enhance the cytotoxicity exhibited by resveratrol itself. Cytotoxicity was found to be due to H_2O_2 produced upon accumulation of the derivatives into mitochondria; ROS-independent mitochondrial depolarization was also induced. We investigate here the mechanisms underlying these effects.

Since effectiveness increased if the two free hydroxyls of the derivatives were acetylated or methylated [13], autooxidation of the polyphenolic nucleus, which depends on the presence of free hydroxyls and is favored by their ionization [15], could be excluded. Oxidation of the resveratrol "kernel" could be ruled out as the source of superoxide also because cyclic voltammetry experiments showed that resveratrol and its mitochondriotropic derivatives are not readily oxidizable at physiologically relevant voltages (Mattarei, A. et al., unpublished results). A protonophoric cycle, such as that envisioned for mitochondriotropic quercetin derivatives [16], can be dismissed as the cause of depolarization because of the lack of proton-carrying groups in the most effective, methylated, molecules. Thus we thought that ROS were likely to be generated downstream of the interaction of our molecules with redox-active proteins. The most likely candidates were components of the respiratory chain. Indeed some evidence for a modulation of respiratory chain complexes by resveratrol has already been presented [17,18].

Ca^{2+} is a major second messenger modulating many cellular physiological functions. Calcium and ROS are linked by a reciprocal interaction: Ca^{2+} overload may cause ROS generation [19], and in turn ROS may have an impact on Ca^{2+} homeostasis. Acute as well as chronic oxidative stress can result in inhibition/downregulation/modulation of the plasma membrane Ca^{2+} ATPase, reticular Ca^{2+} ATPase, Na^+/Ca^{2+} exchanger, and other components of the Ca^{2+} homeostasis machinery [20]. Depending on ROS levels, these effects may be mediated by the action of redox-sensitive kinases, by direct modification of the "pumps" and transporters, or both [21].

Resveratrol is furthermore known to bind to the F_1 portion of the mitochondrial ATP synthase inhibiting the enzyme [22–24]. We therefore focused on Ca^{2+} levels and on ATPase functionality as well as on respiration and ROS production.

2. Materials and methods

Experiments were repeated at least three times. Averages ± s.d. are reported.

2.1. Materials

Resveratrol was purchased from Waseta Int. Trading Co. (Shanghai, P.R. China). R-4′BTPI, R-3BTPI, RDA-4′BTPI, RDA-3BTPI, RDM-4′BTPI and RDM-3BTPI were synthesized as described in [12,13]. Other chemicals were purchased from Sigma-Aldrich (Milan) unless otherwise specified. All chemicals for buffer preparation were of laboratory grade, obtained from Merck, J.T. Baker or Sigma.

2.2. Cells and mitochondria

Mouse colon cancer CT-26 cells (doubling time 24 h) were grown in high glucose (4.5 g/L) Dulbecco's Modified Eagle Medium (DMEM) supplemented with 10% (v/v) fetal bovine serum (FBS, Invitrogen), 10 mM HEPES buffer (pH 7.4), 1 mM sodium pyruvate, 100 U/mL penicillin G, 0.1 mg/mL streptomycin, 2 mM glutamine (GIBCO) and 1% nonessential amino acids (100× solution; GIBCO), in a humidified atmosphere of 5% CO_2 at 37 °C.

Rat liver mitochondria (RLM) were isolated by conventional differential centrifugation procedures [25]. The standard isolation medium was: 250 mM sucrose, 5 mM HEPES, 1 mM EGTA (pH 7.4). Protein content was quantified with a BCA Protein Assay Kit (Thermo Scientific) using an albumin calibration curve.

2.3. Fluorescence microscopy

An Olympus Biosystems apparatus comprising an Olympus IX71 microscope and MT20 light source was used; images were acquired automatically at 1-min intervals for 70 min, and processed with CellR® software. CT-26 cells were seeded on a XF24-well microplate at a density of 5×10^4 cells/well in DMEM + FBS 10% (200 μL) and incubated overnight in a humidified atmosphere with 5% CO_2 at 37 °C. Cells were then washed with HBSS (in mM units: NaCl 136.9, KCl 5.36, $CaCl_2$ 1.26, $MgSO_4$ 0.81, KH_2PO_4 0.44, Na_2HPO_4 0.34, glucose 5.55, pH 7.4 with NaOH) and loaded with dye. All experiments were performed in DMEM without Phenol red and FBS, at room temperature.

2.3.1. Intracellular Ca^{2+} levels

The non-ratiometric dye Fluo-4 was used to follow [Ca^{2+}] changes in cultured cells under the same experimental conditions used in oxygen consumption assays. Cells were loaded with 20 nM Fluo-4 methyl ester, in the presence of 0.04% Pluronic acid, 100 μM Probenecid and 2 μM CsA, at 37 °C for 30 min. The medium was then replaced with 670 μL of pre-warmed (37 °C) DMEM supplemented with 0.04% Pluronic acid, 100 μM Probenecid and 2 μM CsA; cells were then incubated for 30 min at 37 °C to allow complete hydrolysis of Fluo-4 ester bonds. Excitation wavelength was 480–500 nm and fluorescence was collected at $\lambda > 510$ nm. Additions were performed by withdrawing 0.5 mL of incubation medium, adding to this aliquot the desired compound as a solution in 70 μL of DMEM and adding back the solution into the chamber at a peripheral point.

2.3.2. $O_2^{-\bullet}$ generation

$O_2^{-\bullet}$ generation in cells was followed using MitoSOX Red™ (Life Technologies). CT-26 cells were loaded with 1 μM MitoSOX Red™, in the presence of 2 μM CsA, at 37 °C for 30 min. The medium was then replaced with 670 μL of pre-warmed (37 °C) DMEM containing 2 μM CsA. Excitation was at 500–520 nm, and fluorescence was collected at $\lambda > 570$ nm. Additions were performed as described above.

2.4. Oxygen consumption assay by CT-26 cells

Respiration by adherent cells was measured using a Seahorse XF24 (Seahorse Bioscience) which measures the oxygen consumption rate (OCR) in the medium immediately surrounding adherent cells cultured in an XF24-well microplate. Adherent CT-26 cells were seeded at a density of 5×10^4 cells/well in DMEM + FBS 10% (200 μL) and incubated overnight in a humidified atmosphere with 5% CO_2 at 37 °C. The medium was then replaced with 670 μL of pre-warmed (37 °C) high-glucose DMEM supplemented with 1 mM sodium pyruvate, 4 mM L-glutamine, and without FBS. Microplates were incubated at 37 °C for 30 min to allow temperature and pH to stabilize before the measurements. OCR was measured at preset time intervals while the instrument automatically carried out the pre-programmed additions of the various compounds (final concentrations unless otherwise specified: oligomycin A 1 μg/mL, FCCP 0.2 μM, antimycin A 1 μM), added as a solution in 70 μL of DMEM. All measurements were carried out in quadruplicate (4 wells per condition). For presentation purposes the data were normalized to the initial OCR baseline measurement for each set of wells and are presented as % changes with respect to that level. ECAR (extracellular acidification rate) was also automatically measured during the same experiments.

2.5. Activity of mitochondrial respiratory chain complexes

Complex activity was extrapolated from the slope of absorbance decrease; data are expressed as % of the control (i.e., the activity without any addition of the derivative).

2.5.1. Complex I activity

To assay NADH-CoQ oxidoreductase (complex I) activity, RLM (50 μg prot./mL) were incubated with 10 μM alamethicin, 3 mg/mL bovine serum albumin (BSA), 10 mM Tris–HCl (pH 8.0), 2.5 mM NaN_3 and 65 μM coenzyme Q_1 (CoQ_1). The reaction was started with the addition of 100 μM NADH. Changes in absorbance (340 nm) were monitored at 37 °C using an Agilent Technologies Cary 100 UV–Vis spectrophotometer. After 6 min, 2 μM rotenone was added to assess the rotenone- (and thus complex I-) independent activity to be subtracted.

2.5.2. Complex II activity

To measure succinate CoQ oxidoreductase (complex II) activity, RLM (5 μg prot./mL) were incubated in the assay medium (potassium phosphate 25 mM, pH 7.5, supplemented with 5 mM $MgCl_2$, 20 mM succinate and 10 μM alamethicin) at 30 °C for 10 min. 3 mg/mL BSA, 2.5 mM NaN_3, 2 μg/mL antimycin A, 2 μM rotenone, and 125 μM 2,6-dichlorophenolindophenol (DCPI) were then added and absorbance changes were monitored at 600 nm.

2.5.3. Complex III activity

To assay CoQ cytochrome *c* oxidoreductase (complex III) activity, RLM (10 μg prot./mL) were added to a cuvette containing 50 mM potassium phosphate buffer, pH 7.5, supplemented with 10 μM alamethicin, 3 mg/mL BSA, 2.5 mM NaN_3, 2 μM rotenone, 0,025% TWEEN, and 75 μM oxidized cytochrome *c*. The reaction was started adding 75 μM of reduced decylubiquinol (produced by reduction of decylubiquinone in ethanol with $NaBH_4$ shortly before use); changes in absorbance were monitored at 550 nm, 37 °C. After 6 min, 2 μg/mL antimycin was added for assessment of the antimycin-dependent complex III enzyme activity.

2.6. F_0F_1 ATPase activity

Mitochondrial F_0F_1 ATPase activity was measured by coupling the production of ADP to the oxidation of NADH via the pyruvate kinase and lactate dehydrogenase reaction (coupled assay), as described in [26]. The reaction mixture (pH 7.6) contained 250 mM sucrose, 10 mM Tris–HCl, 200 μM EGTA–Tris, 1 mM NaH_2PO_4, 6 mM $MgCl_2$, 2 μM rotenone, 10 μM alamethicin, 3 mg/mL BSA, 1 mM phosphoenolpyruvate (PEP), 0.1 mM NADH, pyruvate kinase (PK; 20 units/mL), lactate dehydrogenase (LDH; 50 units/mL), and RLM (20 μg prot./mL). Absorbance was measured at 340 nm, 25 °C. The reaction was started by the addition of 500 μM ATP; after 6 min, 1 μg/mL oligomycin A was added to evaluate F_0F_1-ATPase-independent ATP hydrolysis.

3. Results

Since H_2O_2 is responsible for cell death induction by mitochondriotropic resveratrol derivatives [13], the mechanisms underlying ROS generation were investigated using cultured cells and isolated rat liver mitochondria. All tested compounds are illustrated in Fig. 1; both isomers were used, bearing the 4-triphenylphosphoniumbutyl (BTPI) group at either position -3 or -4′.

3.1. Effects on intracellular Ca^{2+} levels. Ca^{2+} signalling does not have a role in cytotoxicity

Since ROS and Ca^{2+} signalling can be linked [19–21], we evaluated the effects of treatment with the most cytotoxic compounds, RDM-3BTPI and RDM-4′BTPI (5 μM), on CT-26 cellular Ca^{2+} levels. The two isomers had very similar effects; observations obtained with RDM4′-BTPI are illustrated in Fig. 2A–C. The Ca^{2+} probe Fluo-4 was used in fluorescence microscopy experiments conducted under the same conditions used in the experiments on cellular respiration (SeaHorse; see Section 3.3). Ionomycin was used as a control to make sure that the Fluo-4 probe was responding adequately to Ca^{2+}, and to determine the maximum Fluo-4 fluorescence response. In control experiments (i.e., untreated cells), less than 1% of the cell population displayed sporadic (generally one or two per cell) brief (≤1 min) increases of intracellular [Ca^{2+}] during the one-hour monitoring period. The effect of the resveratrol derivatives was to increase from <1% to ~5% the fraction of cells displaying these [Ca^{2+}] "spikes". These occurred randomly, but with a preference for late times after addition of the derivative (>40 min). They did not impair the ability of the cell to take up Ca^{2+} upon the introduction of ionomycin at the end of the experiment.

Occurrence of the [Ca^{2+}] transients was not downstream of ROS production, since the presence of PEG-SOD and PEG-CAT had no effect on their prevalence, intensity or multiplicity (Fig. 2C). PEG-SOD and PEG-CAT were proven, however, to efficiently reduce ROS generation under these same experimental conditions (Fig. 2F).

Superoxide production was observed in fluorescence microscopy experiments using the MitoSOX™ probe (Fig. 2D–F). Under the same experimental conditions as in Fig. 2A–C, superoxide generation increased in all cells (Supplementary Fig. 1), beginning shortly after the addition of the mitochondriotropic derivatives (Fig. 2D). On the other hand, brief calcium spikes occurred only in a small fraction of cells, and with a random delay after compound addition (Fig. 2B and C). The comparison of the time course and prevalence of the two phenomena allows one to conclude that ROS production was not downstream of the modest Ca^{2+} signals. Note that the response elicited by antimycin A (Fig. 2E) was similar to that caused by RDM-4′BTPI (Fig. 2D), and that the two were not additive (Fig. 2D). The presence of cell-permeant PEG-SOD and PEG-CAT eliminated the MitoSOX™ fluorescence increase elicited by RDM-4′BTPI (Fig. 2F), confirming on one side that it is due to mitochondrial ROS, and on the other that the enzymes added effectively scavenge $O_2^{\bullet}/H_2O_2$. The behavior shown in Fig. 2F is completely analogous to that exhibited by MitoSOX™-loaded but otherwise untreated (control) cells (not shown).

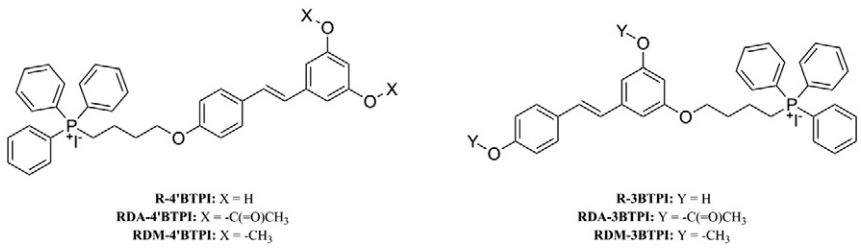

Fig. 1. Mitochondriotropic resveratrol derivatives studied.

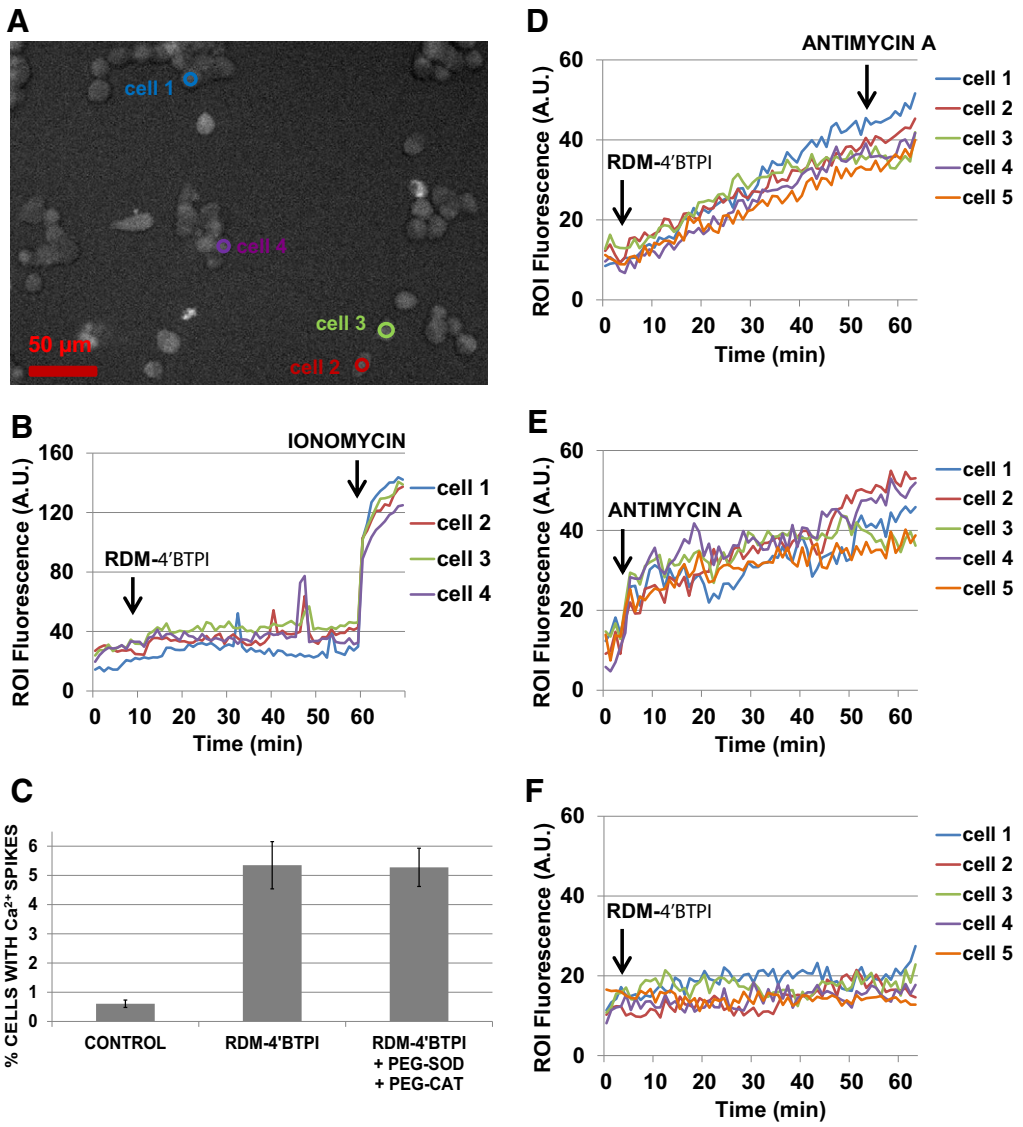

Fig. 2. Effects of RDM-4′BTPI on intracellular Ca^{2+} levels (A–C) and $O_2^{-\bullet}$ generation (D–F). A–C: Fluorescence microscopy experiments with Fluo-4 loaded CT-26 cells. A: an image (λ_{exc}: 492 nm; $\lambda_{em} > 510$ nm) acquired 30 min after addition of 5 μM RDM-4′BTPI; B: computer-generated plots of the fluorescence emitted by the regions of interest (ROI) identified in panel A, with background subtraction. The behavior of 4 cells displaying Ca^{2+} spikes is reported. 5 μM RDM-4′BTPI and 2.5 μM ionomycin were added when indicated. C: Overall extent of the phenomenon, expressed as % of cells exhibiting $[Ca^{2+}]$ spikes within 1 h, out of the total cell population. Averages ± s.d. are reported. D–F: Fluorescence microscopy experiments with MitoSOX™-loaded CT-26 cells. Computer-generated plots of the fluorescence emitted by some regions of interest (ROI); each ROI was selected to enclose one cell. The behavior of 5 representative cells is reported. 5 μM RDM-4′BTPI and/or 1 μg/mL antimycin A were added when indicated. F: PEG-SOD (40 U/mL) and PEG-CAT (500 U/mL) were present from the beginning.

3.2. Interactions with the respiratory chain

A possible rationalization of superoxide generation by our derivatives is that they may interfere with respiration, diverting part of the electron flow to superoxide production. We verified their effect on the rate of fully uncoupled (by FCCP) respiration by CT-26 cells; a high concentration (50 μM) was used, to roughly compensate for the lack of accumulation due to the dissipation of the transmembrane potential by FCCP. The compounds did decrease the rate of oxygen consumption (Fig. 3); this indicates that they can interact with respiratory chain components. This interaction seems to be favored by "masking" of the free hydroxyls with methyl or acetyl groups. Resveratrol itself caused only a modest inhibition, while rotenone and antimycin produced the expected drastic respiratory decrease, similar in extent to that observed with RDM-BTPIs (Supplementary Fig. 2).

To confirm respiratory chain inhibition and ROS generation by mitochondria we performed measurements of oxygen consumption and ROS generation with isolated rat liver mitochondria (RLM). The experiments confirmed the inhibitory effect on respiration driven by complex I (glutamate/malate) or complex II (succinate/rotenone) substrates. FACS analysis of isolated rat liver mitochondria loaded with H_2DCF-DA confirmed that our compounds cause ROS production by mitochondria energized either via complex I or complex II (Supplementary Fig. 3).

We thus verified the effect of our derivatives on the activity of the individual complexes, using alamethicin-permeabilized RLM. Also in this case, to roughly simulate the concentration of mitochondriotropic derivatives in the presence of a $\Delta\psi_m$ (which in these experiments was dissipated by permeabilization), the compounds were also used at 50 μM (Fig. 4B). Under these latter conditions inhibition of respiratory chain complexes was found to be significant in most cases, as assessed by the Mann–Whitney test. The observed effects however differed considerably in magnitude; we focus here only on the most significant ones (i.e. those inducing at least 30% activity inhibition). Complexes I and III were particularly inhibited, and methylated derivatives were the most

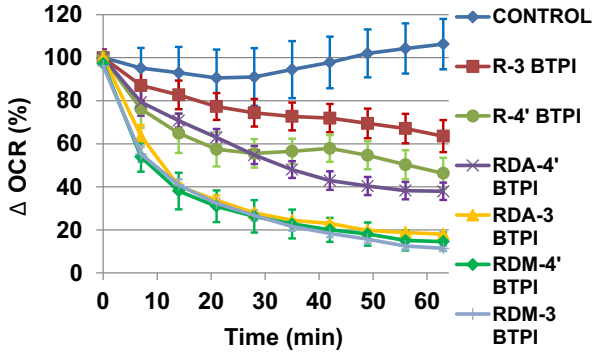

Fig. 3. Effect of mitochondriotropic resveratrol derivatives on the rate of respiration fully stimulated by FCCP. Rates of respiration by CT-26 cells were determined using a Seahorse XF24. Representative experiments are shown. Derivatives (50 μM) were added to cells after 0.2 μM FCCP. Data were normalized to the initial FCCP-elicited OCR for each set of wells and are presented as % changes with respect to that level.

effective (Fig. 4). They partially inhibited complex I (RDM-4′BTPI only) and complex III (both isomers) even at 5 μM (Fig. 4A). Resveratrol itself was shown to significantly inhibit only complex I, and only when used at 50 μM. This effect is much weaker compared to the inhibitory effects obtained with acetylated or methylated mitochondriotropic derivatives at the same concentration (about 20% inhibition vs 60–90% inhibition).

3.3. Effects on cellular oxygen consumption

5 μM R-3BTPI or R-4′BTPI had little effect on the rate of oxygen consumption by otherwise untreated CT-26 cells in experiments with Seahorse XF24 (Fig. 5A). Under the same experimental conditions, only RDM-4′BTPI reduced respiration (Fig. 5C), while RDA-3BTPI, RDA-4′BTPI and RDM-3BTPI induced relatively minor perturbations (Fig. 5B, C). However, all these four compounds drastically reduced the respiratory response to the subsequent addition of oligomycin and FCCP (Fig. 5A–C). A massive loss of cells due to death and detachment was excluded by direct microscopic observation of the cells at the end of the experiments. On the other hand, if the respiration rate was first reduced using the ATP synthase inhibitor oligomycin A, the subsequent addition of RDA-3BTPI, RDA-4′BTPI, RDM-3BTPI or RDM-4′BTPI induced an increase in oxygen consumption (respiratory "recovery"), which could hardly be further increased by the uncoupler FCCP, but was sensitive to antimycin A, an inhibitor of the mitochondrial respiratory chain (complex III) (Fig. 5E, F), thus confirming that the increase was due to respiration. R-3BTPI and R-4′BTPI had little effect in this experimental setup as well (Fig. 5D). Respiration rates in the presence of both the mitochondriotropic derivative and oligomycin were, as may be expected, similar irrespective of the order of addition.

Given the presence of oligomycin and the known interaction of resveratrol with the mitochondrial F_0F_1 ATP synthase [24,27], we initially hypothesized that the synthase may have a role in the respiratory recovery, and verified whether the compounds might be competing with oligomycin, displacing it and re-activating the enzyme. However, increasing oligomycin dosages did not prevent or markedly reduce the extent of the recovery; rather, with high oligomycin (3 or 10 μg/mL) there was a subsequent decline of the rate of respiration (Fig. 6 and Supplementary Fig. 4), which could not be rescued by FCCP, while antimycin A inhibited what respiration was left. The higher the dose of oligomycin, the more pronounced this second-stage respiratory decline, which was furthermore not affected by elimination of H_2O_2 with PEG-CAT (Supplementary Fig. 4). High concentrations of oligomycin alone caused the expected decrease of cellular respiration, which remained depressed indefinitely, without any recovery resembling that observed upon the further addition of an acylated or methylated mitochondriotropic resveratrol derivative.

The behaviour elicited by RDM-4′BTPI was again, to an extent, discrepant. With this compound the respiratory recovery in the presence of oligomycin was less pronounced than with the other compounds (Fig. 5F), and oxygen consumption after the recovery in the presence of high oligomycin declined less markedly (Fig. 6). RDM-4′BTPI is the most powerful inhibitor of complex I (Fig. 4) and the only compound which decreased OCR by untreated cells at the 5 μM level (Fig. 5C). The lower extent of respiratory recovery might thus be due to a more pronounced inhibition of the respiratory chain.

The secondary decrease of oxygen consumption at high oligomycin dosages is reminescent of an analogous phenomenon which often follows induction of the mitochondrial permeability transition (MPT), and is attributed to loss of respiratory intermediates via the MPT pore. We thus performed the same experiments in the presence of CsA, and found that the oxygen consumption rate was partially rescued by CsA when high oligomycin concentrations were used, indicating that the MPT may indeed be taking place and may at least partially account for the observations (Fig. 6). The effect is particularly evident in the case of derivatives bearing the -BTPI at position -3 of the stilbene skeleton (RDA-3BTPI and RDM-3BTPI) (Fig. 6A and C). On the other hand, we confirmed that MPT was not involved in cell death induced by our compounds alone, since CsA had no impact on the readout of MTT assays (Supplementary Fig. 5).

3.4. Interactions with the F_0F_1 ATP synthase

The effect of high oligomycin suggests an involvement of the F_0F_1 ATP synthase. Indeed, resveratrol itself is known to bind to the F_1 portion of this multimeric enzyme complex [24]. We checked the effect of the resveratrol derivatives on the hydrolytic activity of the RLM ATP synthase. Experiments were performed using isolated RLM in the

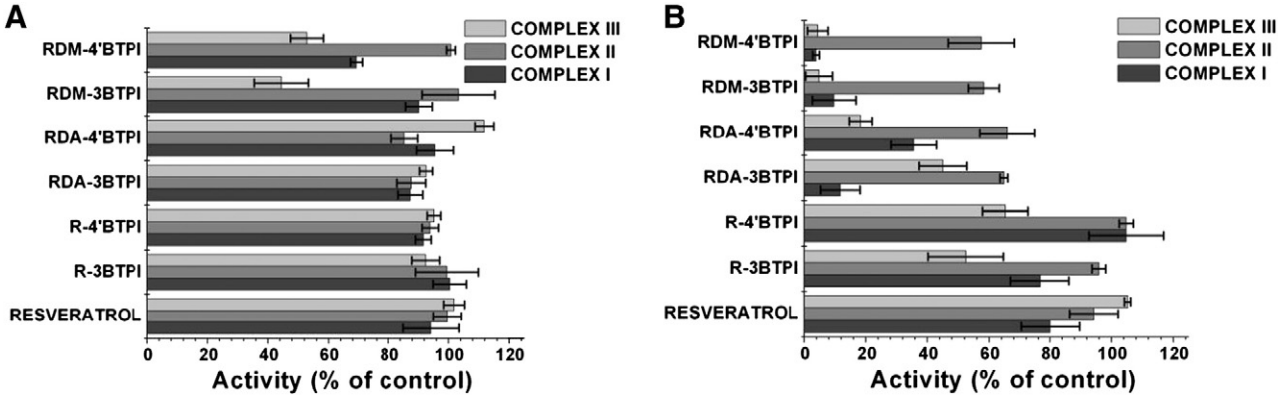

Fig. 4. Effects of resveratrol and its mitochondriotropic derivatives on the activity of the indicated respiratory chain complexes, in permeabilized RLM. Averages ± s.d. are reported (N = 3). Concentration of the derivatives was 5 μM (A) or 50 μM (B).

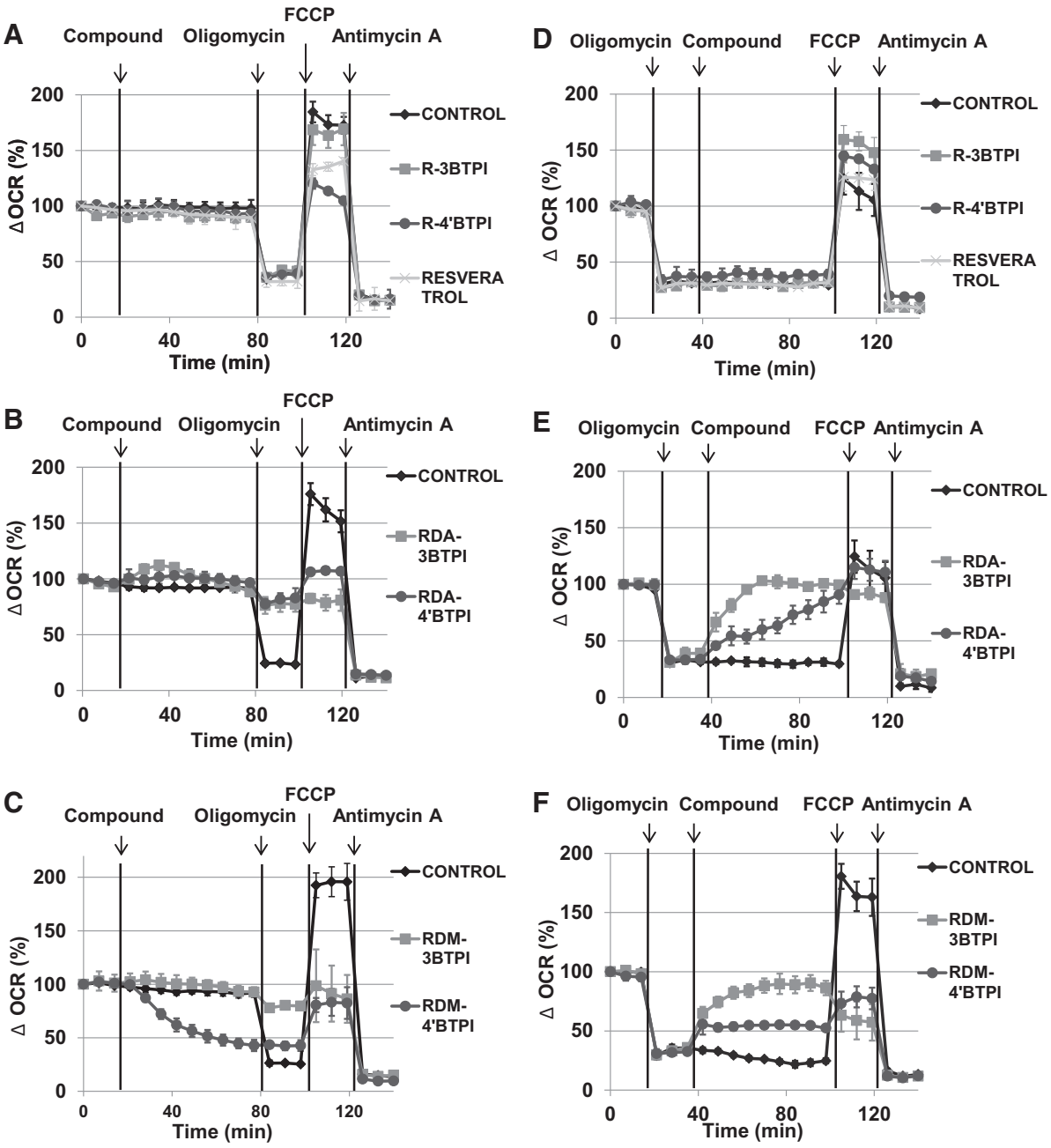

Fig. 5. Effects of mitochondriotropic resveratrol derivatives on the respiration of cultured cells. Rate of respiration by CT-26 cells as determined using Seahorse XF24. Representative experiments are shown. 5 μM of the indicated compounds was added to cells before (A, B, C) or after (D, E, F) the addition of 1 μg/mL oligomycin. A, D: resveratrol and non-acetylated/methylated derivatives; B, E: acetylated derivatives; C, F: methylated derivatives.

presence of alamethicin, which completely permeabilizes membranes to externally added reagents and also causes complete depolarization. Acetylated and methylated derivatives, as well as resveratrol, turned out to be inhibitors of the ATPase at 50 μM, while R-3BTPI and R-4′ BTPI did not (Fig. 7).

ATPase inhibition by RDA-BTPIs and RDM-BTPIs was associated with an increase in the glycolytic activity of the cells, as shown by increased extracellular acidification rate (ECAR) after addition of RDA- or RDM-BTPIs (Supplementary Fig. 6).

4. Discussion

In our previous work with mitochondriotropic resveratrol derivatives [13] we had established that cell death is caused by H_2O_2, generated following accumulation of the compounds in mitochondria. Data presented above confirm this, indicating that cell death is not a consequence of Ca^{2+} dysregulation (Fig. 2) or of MPT occurrence (Supplementary Fig. 5). The compounds did increase the (low) probability of observing transient [Ca^{2+}] "spikes" in treated cells, but a relationship between this increase and the induction of cell death can be excluded because the [Ca^{2+}] spikes remained anyhow rare and were observed only in a small percentage of cells, and because death-abolishing membrane-permeant radical scavangers PEG-SOD + PEG-CAT had no effect on the [Ca^{2+}] transients. Our previous observations [13] had furthermore suggested that superoxide anion, the precursor of H_2O_2, might be formed by "slipping" complexes of the respiratory chain, which would transfer single electrons to oxygen molecules upon interaction with the compounds. This model is supported by the observation that RDA-BTPIs and RDM-BTPIs inhibit FCCP-uncoupled respiration of CT-26 cells (Fig. 3). More specifically, experiments with RLM indicate that

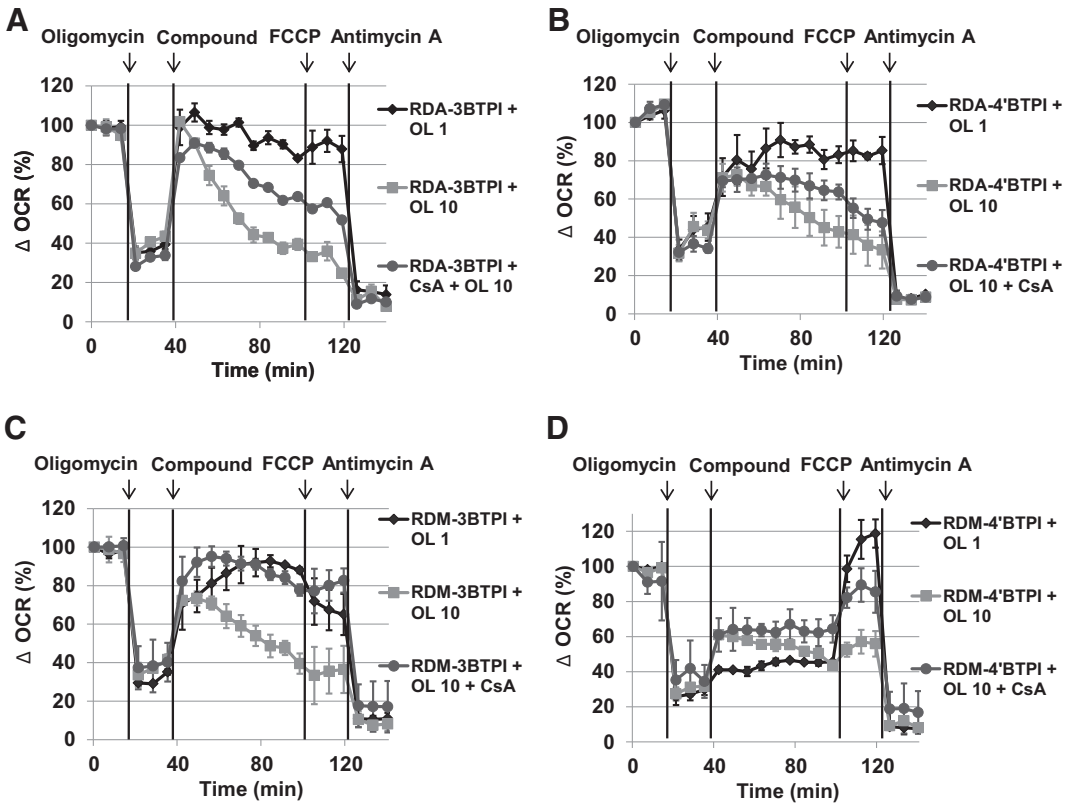

Fig. 6. Acetylated and methylated mitochondriotropic resveratrol derivatives affect respiration in an oligomycin-dependent manner. Rate of respiration by CT-26 cells as determined using Seahorse XF24. Representative experiments are shown. 5 μM of the indicated derivative was added to cells after inhibition of ATP synthase activity with oligomycin 1 μg/mL (OL 1) or 10 μg/mL (OL 10). The effect on respiration of the presence of CsA (2 μM) from the beginning of the experiment is also shown.

complexes I and III are considerably inhibited (Fig. 4). RDM-3BTPI and RDM-4′BTPI are the most powerful inhibitors; they are about equally effective on complex III, while RDM-4′BTPI appears to act more strongly than its isomer on complex I. These two complexes are known to be the major source of ROS in normal respiring mitochondria, and it is plausible that the mitochondriotropic compounds may elicit an increase of this side reaction, analogously to what happens in the case of complex II and vitamin E analogs [28]. The methylated derivatives are also, along with RDA-3BTPI, the most powerful inducers of superoxide production [13]. This correlation between inhibition of respiratory chain complexes and production of superoxide supports the notion that ROS production is a consequence of the interaction of the compounds with the complexes.

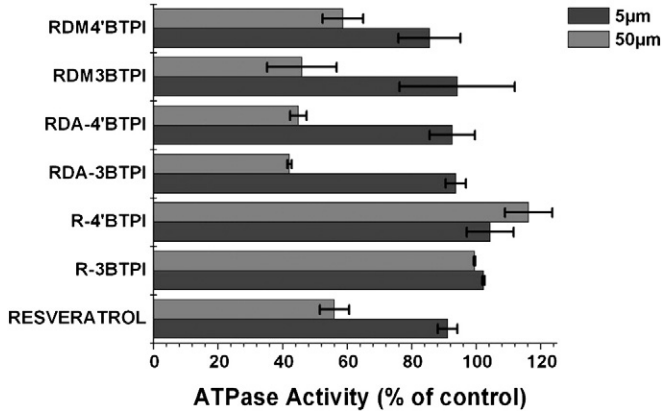

Fig. 7. Effects of resveratrol and its mitochondriotropic derivatives on the rate of ATP hydrolysis by permeabilized RLM. Averages ± s.d. are reported (N = 3).

In the same concentration range, the RLM F_0F_1 ATPase is also inhibited (Fig. 7). The four compounds with all hydroxyls capped by a substituent appear to be about equally effective. Resveratrol and other stilbene derivatives are known to interact with the F_1 portion, binding in a pocket formed by the γ and β_{TP} subunit and thereby blocking rotation ([27] and refs therein).

The higher efficiency of acetylated and methylated compounds as inhibitors and as inducers of ROS production may reflect a better partition into membranes and/or a higher affinity for the enzymes involved (see [29]). Please note that acetylated derivatives may undergo hydrolysis with rates dependent on conditions, regenerating R-3BTPI and R-4′ BTPI [13].

These inhibitory properties largely account for the observations with cultured cells. In this system at least three counteracting effects of our compounds are expected to modulate oxygen consumption: inhibition of the respiratory chain and of the F_0F_1 ATP synthase (which when in operation stimulates respiratory activity via its effects on $\Delta\tilde{\mu}_H$) will tend to lower respiration while dissipation of $\Delta\tilde{\mu}_H$ [13] will tend to increase it. That ATP synthesis is hardly contributing to respiration after a one-hour exposure to 5 μM RDA- and RDM-derivatives is shown by the smallness of the effect of oligomycin (Fig. 5). That respiration is close to having exhausted its "reserve capacity" (e.g. [30]) is indicated by the lack, or near-lack of effect by FCCP (Fig. 5B–C). RDM-4′BTPI is the only compound causing a pronounced decrease of respiration by otherwise untreated CT-26 cells (Fig. 5C). This might in principle be due to a better inhibition of the ATP synthase or to a less pronounced $\Delta\psi_m$ dissipation. The data however rule these hypotheses out (Fig. 7 and [13]), leaving its greater effectiveness as an inhibitor of complex I as the plausible reason.

Measurements of respiratory rates in the presence of variable concentrations of oligomycin A, a polyketide inhibitor of the mitochondrial F_0F_1 ATP synthase acting at the interface between the c-ring and subunit

a [27], point to a further mode of action of the acetylated and in particular of the methylated compounds. If cellular respiration has previously been depressed by oligomycin, their addition induces a recovery of the respiratory rate (Fig. 5E, F). This may be simply a reflection of the loss of $\Delta\psi_m$ induced by them, the mechanism of which remains to be elucidated. By the tenets of the chemiosmotic model, depolarization with associated respiratory stimulation is likely to reflect the appearance of a $\Delta\psi_m$-dissipating proton leak. Since our derivatives interact with respiratory chain complexes and with the ATP synthase, it seems logical to propose that this proton leak may result from a functional uncoupling of the former or, more likely, the latter. In other words, we suggest that binding to complex V our compounds may not only inhibit ATP hydrolysis (and presumably synthesis), but also transform the ATP synthase into a conduit for a proton flux not associated with ATP synthesis/hydrolysis ("intrinsic uncoupling" or "proton slip"). Indeed the ATP synthase has been proposed to be able to conduct a "proton slip", a process possibly induced by isoflurane [31] or 17 β-estradiol [32] and modulated by Bcl-xL [33].

In this context it is of interest that at high oligomycin doses the respiratory recovery is followed by a CsA-sensitive decline (Fig. 6), which suggests the onset, in a stilbenoid-induced and oligomycin-sensitive process, of the permeability transition. By itself, oligomycin decreases cellular respiration due to ATP synthase inhibition, but has no further effects in the concentration range used in this work. In the literature on the MPT oligomycin is considered to be, if anything, a protective agent [34]. It follows that in our experimental system MPT pore opening can be mediated by membrane component(s) sensitive to the presence of both our mitochondriotropic derivatives and oligomycin. It seems logical to think of the ATP synthase. In the presence of excess oligomycin, the putative uncoupling ATP synthase-mediated "proton slip" may become a canonical, CsA-sensitive MPT. That development of the MPT pore may be preceded by a "small pore" phase, in which the membrane is permeable only to small ions, has been proposed in a number of papers [34–38]. It has been recently argued on the basis of electrophysiological and biochemical evidence that the ATP synthase dimer may be responsible for the generation of the MPT pore [39,40]. One point in favor of this model is the fact that the MPT pore has long been proposed to have a dimeric structure on the basis of patch-clamp recordings [34,41,42]. Our observations are therefore coherent with the emerging molecular model of the pore and reinforce it. Fig. 8 presents our working model of the cytotoxic action of mitochondriotropic resveratrol derivatives on cells. Again, while uncoupling and inhibition of the ATP synthase may well be expected to eventually lead to cell death, the most rapidly acting agent is the H_2O_2 produced. We would also like to emphasize that the onset of the MPT is only inferred to take place in our system when excess oligomycin is also provided. Judging from the lack of sensitivity of cell death to CsA (Supplementary Fig. 5), the MPT appears not to be the proximal cause of cell death induction by our mitochondriotropic resveratrol derivatives alone. The latter take in any case a front-line position in the ranks of redox-active potential "mitocans".

Acknowledgments

We thank Prof. P. Bernardi for useful discussions and access to equipment, and Mr. M. Simonetti for help with the artwork. This work was supported by grants from the Fondazione Cassa di Risparmio di Padova e Rovigo (CARIPARO) ("Developing a Pharmacology of Polyphenols"), from the Italian Ministry of the University and Research (PRIN no. 20107Z8XBW_004), and from the CNR Project of Special Interest on Aging.

Appendix A. Supplementary data

Supplementary data to this article can be found online at http://dx.doi.org/10.1016/j.bbabio.2014.06.010.

References

[1] D. Gius, D.R. Spitz, Redox signaling in cancer biology, Antioxid. Redox Signal. 8 (2006) 1249–1252.
[2] D. Trachootham, J. Alexandre, P. Huang, Targeting cancer cells by ROS-mediated mechanisms: a radical therapeutic approach? Nat. Rev. Drug Discov. 8 (2009) 579–591.

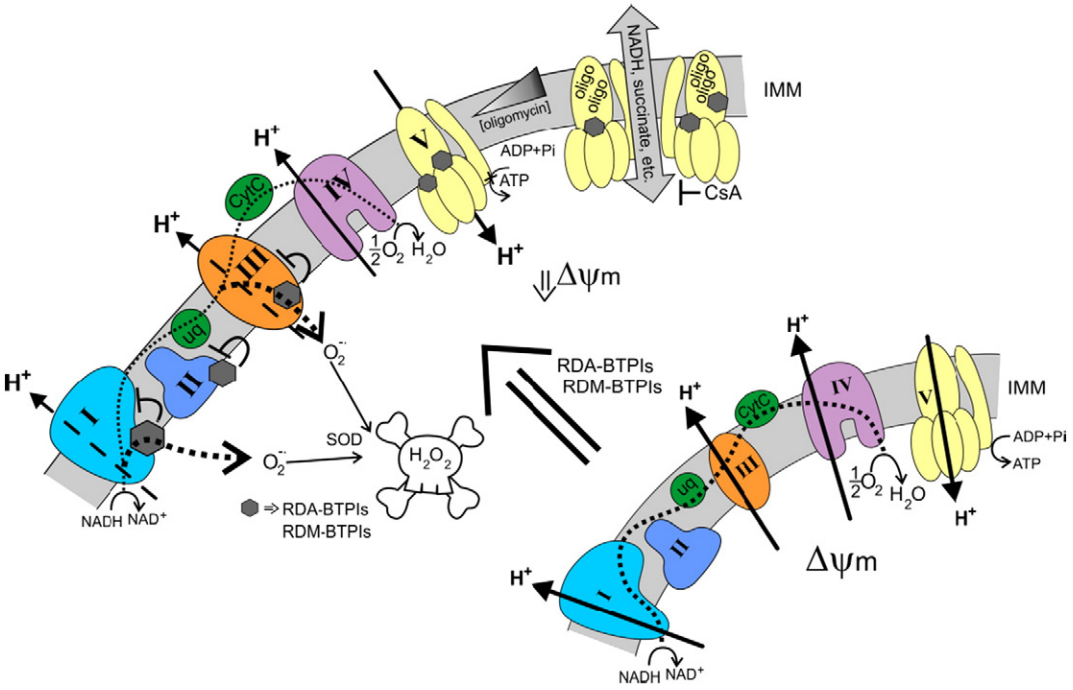

Fig. 8. Proposed mechanisms of cytotoxic action of mitochondriotropic resveratrol derivatives emerging from this work.

[3] S.J. Ralph, S. Rodriguez-Enriquez, J. Neuzil, R. Moreno-Sanchez, Bioenergetic pathways in tumor mitochondria as targets for cancer therapy and the importance of the ROS-induced apoptotic trigger, Mol. Asp. Med. 31 (2010) 29–59.
[4] S.J. Ralph, S. Rodriguez-Enriquez, J. Neuzil, E. Saavedra, R. Moreno-Sanchez, The causes of cancer revisited: "mitochondrial malignancy" and ROS-induced oncogenic transformation — why mitochondria are targets for cancer therapy, Mol. Asp. Med. 31 (2010) 145–170.
[5] L. Leanza, L. Trentin, K.A. Becker, F. Frezzato, M. Zoratti, G. Semenzato, E. Gulbins, I. Szabo, Clofazimine, Psora-4 and PAP-1, inhibitors of the potassium channel Kv1.3, as a new and selective therapeutic strategy in chronic lymphocytic leukemia, Leukemia 27 (2013) 1782–1785.
[6] J.S. Modica-Napolitano, J.R. Aprille, Delocalized lipophilic cations selectively target the mitochondria of carcinoma cells, Adv. Drug Deliv. Rev. 49 (2001) 63–70.
[7] V.R. Fantin, M.J. Berardi, L. Scorrano, S.J. Korsmeyer, P. Leder, A novel mitochondriotoxic small molecule that selectively inhibits tumor cell growth, Cancer Cell 2 (2002) 29–42.
[8] S. Bonnet, S.L. Archer, J. Allalunis-Turner, A. Haromy, C. Beaulieu, R. Thompson, C.T. Lee, G.D. Lopaschuk, L. Puttagunta, S. Bonnet, G. Harry, K. Hashimoto, C.J. Porter, M.A. Andrade, B. Thebaud, E.D. Michelakis, A mitochondria-K + channel axis is suppressed in cancer and its normalization promotes apoptosis and inhibits cancer growth, Cancer Cell 11 (2007) 37–51.
[9] S.H. Dairkee, A.J. Hackett, Differential retention of rhodamine 123 by breast carcinoma and normal human mammary tissue, Breast Cancer Res. Treat. 18 (1991) 57–61.
[10] J. Neuzil, L.F. Dong, J. Rohlena, J. Truksa, S.J. Ralph, Classification of mitocans, anti-cancer drugs acting on mitochondria, Mitochondrion 13 (2013) 199–208.
[11] L. Biasutto, L.F. Dong, M. Zoratti, J. Neuzil, Mitochondrially targeted anti-cancer agents, Mitochondrion 10 (2010) 670–681.
[12] L. Biasutto, A. Mattarei, E. Marotta, A. Bradaschia, N. Sassi, S. Garbisa, M. Zoratti, C. Paradisi, Development of mitochondria-targeted derivatives of resveratrol, Bioorg. Med. Chem. Lett. 18 (2008) 5594–5597.
[13] N. Sassi, A. Mattarei, M. Azzolini, P. Bernardi, I. Szabo, C. Paradisi, M. Zoratti, L. Biasutto, Mitochondria-targeted resveratrol derivatives act as cytotoxic pro-oxidants, Curr. Pharm. Des. 20 (2014) 172–179.
[14] D. Delmas, E. Solary, N. Latruffe, Resveratrol, a phytochemical inducer of multiple cell death pathways: apoptosis, autophagy and mitotic catastrophe, Curr. Med. Chem. 18 (2011) 1100–1121.
[15] G. Cao, E. Sofic, R.L. Prior, Antioxidant and prooxidant behavior of flavonoids: structure–activity relationships, Free Radic. Biol. Med. 22 (1997) 749–760.
[16] L. Biasutto, N. Sassi, A. Mattarei, E. Marotta, P. Cattelan, A. Toninello, S. Garbisa, M. Zoratti, C. Paradisi, Impact of mitochondriotropic quercetin derivatives on mitochondria, Biochim. Biophys. Acta 1797 (2010) 189–196.
[17] V. Desquiret-Dumas, N. Gueguen, G. Leman, S. Baron, V. Nivet-Antoine, S. Chupin, A. Chevrollier, E. Vessieres, A. Ayer, M. Ferre, D. Bonneau, D. Henrion, P. Reynier, V. Procaccio, Resveratrol induces a mitochondrial complex I-dependent increase in NADH oxidation responsible for sirtuin activation in liver cells, J. Biol. Chem. 288 (2013) 36662–36675.
[18] R. Zini, C. Morin, A. Bertelli, A.A. Bertelli, J.P. Tillement, Effects of resveratrol on the rat brain respiratory chain, Drugs Exp. Clin. Res. 25 (1999) 87–97.
[19] T.I. Peng, M.J. Jou, Oxidative stress caused by mitochondrial calcium overload, Ann. N. Y. Acad. Sci. 1201 (2010) 183–188.
[20] A.V. Zima, L.A. Blatter, Redox regulation of cardiac calcium channels and transporters, Cardiovasc. Res. 71 (2006) 310–321.
[21] S. Wagner, A.G. Rokita, M.E. Anderson, L.S. Maier, Redox regulation of sodium and calcium handling, Antioxid. Redox Signal. 18 (2013) 1063–1077.
[22] J. Zheng, V.D. Ramirez, Inhibition of mitochondrial proton F0F1-ATPase/ATP synthase by polyphenolic phytochemicals, Br. J. Pharmacol. 130 (2000) 1115–1123.
[23] J.R. Gledhill, J.E. Walker, Inhibition sites in F1-ATPase from bovine heart mitochondria, Biochem. J. 386 (2005) 591–598.
[24] J.R. Gledhill, M.G. Montgomery, A.G. Leslie, J.E. Walker, Mechanism of inhibition of bovine F1-ATPase by resveratrol and related polyphenols, Proc. Natl. Acad. Sci. U. S. A. 104 (2007) 13632–13637.
[25] C. Frezza, S. Cipolat, L. Scorrano, Organelle isolation: functional mitochondria from mouse liver, muscle and cultured fibroblasts, Nat. Protoc. 2 (2007) 287–295.
[26] A. Mattarei, L. Biasutto, E. Marotta, U. De Marchi, N. Sassi, S. Garbisa, M. Zoratti, C. Paradisi, A mitochondriotropic derivative of quercetin: a strategy to increase the effectiveness of polyphenols, Chembiochem 9 (2008) 2633–2642.
[27] S. Hong, P.L. Pedersen, ATP synthase and the actions of inhibitors utilized to study its roles in human health, disease, and other scientific areas, Microbiol. Mol. Biol. Rev. 72 (2008) 590–641 (Table of Contents).
[28] S.J. Ralph, R. Moreno-Sanchez, J. Neuzil, S. Rodriguez-Enriquez, Inhibitors of succinate: quinone reductase/complex II regulate production of mitochondrial reactive oxygen species and protect normal cells from ischemic damage but induce specific cancer cell death, Pharm. Res. 28 (2011) 2695–2730.
[29] J. Xiao, G. Kai, A review of dietary polyphenol–plasma protein interactions: characterization, influence on the bioactivity, and structure–affinity relationship, Crit. Rev. Food Sci. Nutr. 52 (2012) 85–101.
[30] B.E. Sansbury, S.P. Jones, D.W. Riggs, V.M. Darley-Usmar, B.G. Hill, Bioenergetic function in cardiovascular cells: the importance of the reserve capacity and its biological regulation, Chem. Biol. Interact. 191 (2011) 288–295.
[31] D. Pravdic, N. Hirata, L. Barber, F. Sedlic, Z.J. Bosnjak, M. Bienengraeber, Complex I and ATP synthase mediate membrane depolarization and matrix acidification by isoflurane in mitochondria, Eur. J. Pharmacol. 690 (2012) 149–157.
[32] A.J. Moreno, P.I. Moreira, J.B. Custodio, M.S. Santos, Mechanism of inhibition of mitochondrial ATP synthase by 17beta-estradiol, J. Bioenerg. Biomembr. 45 (2013) 261–270.
[33] K.N. Alavian, H. Li, L. Collis, L. Bonanni, L. Zeng, S. Sacchetti, E. Lazrove, P. Nabili, B. Flaherty, M. Graham, Y. Chen, S.M. Messerli, M.A. Mariggio, C. Rahner, E. McNay, G.C. Shore, P.J. Smith, J.M. Hardwick, E.A. Jonas, Bcl-xL regulates metabolic efficiency of neurons through interaction with the mitochondrial F_1F_O ATP synthase, Nat. Cell Biol. 13 (2011) 1224–1233.
[34] M. Zoratti, I. Szabo, The mitochondrial permeability transition, Biochim. Biophys. Acta 1241 (1995) 139–176.
[35] S.A. Novgorodov, T.I. Gudz, Permeability transition pore of the inner mitochondrial membrane can operate in two open states with different selectivities, J. Bioenerg. Biomembr. 28 (1996) 139–146.
[36] F. Ichas, J.P. Mazat, From calcium signaling to cell death: two conformations for the mitochondrial permeability transition pore Switching from low- to high-conductance state, Biochim. Biophys. Acta 1366 (1998) 33–50.
[37] Y.E. Kushnareva, P.M. Sokolove, Prooxidants open both the mitochondrial permeability transition pore and a low-conductance channel in the inner mitochondrial membrane, Arch. Biochem. Biophys. 376 (2000) 377–388.
[38] A. Toninello, M. Salvi, M. Schweizer, C. Richter, Menadione induces a low conductance state of the mitochondrial inner membrane sensitive to bongkrekic acid, Free Radic. Biol. Med. 37 (2004) 1073–1080.
[39] V. Giorgio, S. von Stockum, M. Antoniel, A. Fabbro, F. Fogolari, M. Forte, G.D. Glick, V. Petronilli, M. Zoratti, I. Szabo, G. Lippe, P. Bernardi, Dimers of mitochondrial ATP synthase form the permeability transition pore, Proc. Natl. Acad. Sci. U. S. A. 110 (2013) 5887–5892.
[40] P. Bernardi, The mitochondrial permeability transition pore: a mystery solved? Front. Physiol. 4 (2013) 95.
[41] I. Szabo, M. Zoratti, The mitochondrial permeability transition pore may comprise VDAC molecules. I. Binary structure and voltage dependence of the pore, FEBS Lett. 330 (1993) 201–205.
[42] U. De Marchi, I. Szabo, G.M. Cereghetti, P. Hoxha, W.J. Craigen, M. Zoratti, A maxi-chloride channel in the inner membrane of mammalian mitochondria, Biochim. Biophys. Acta 1777 (2008) 1438–1448.